Biochemical and Biophysical Research Communications 410 (2011) 75–80

Contents lists available at ScienceDirect

Biochemical and Biophysical Research Communications

journal homepage: www.elsevier.com/locate/ybbrc

Role of aromatic stack pairing at the catalytic site of gelonin protein

Shashank Prakash Katiyar, Dhamodharan Bakkiyaraj, Shunmugiah Karutha Pandian *

Department of Biotechnology, Alagappa University, Karaikudi 630003, Tamil Nadu, India

ARTICLE INFO

Article history:
Received 16 May 2011
Available online 25 May 2011

Keywords:
Aromatic stack pairing
Ribosome inactivating protein
Gelonin
Mutagenesis
RMSD
Molecular dynamics

ABSTRACT

Aromatic–aromatic interactions play an important role in the enzyme–substrate recognition mechanism and in stabilization of proteins. Gelonin – a ribosome inactivating protein (RIP) from the plant *Gelonium multiflorum* – belongs to type-I RIPs and shows N-glycosylation activity which has been used as a model to explain the role of aromatic–aromatic stack pairing in RIPs. RIPs have a different substrate binding site and catalytic site. Role of tyrosine residues at the binding site has already been known but the role of tyrosine residues at catalytic site is still unclear. In this study, the role of tyrosine–adenine–tyrosine aromatic stack pairing at the catalytic site was studied by *in silico* mutation studies using molecular dynamic simulations. Through this study we report that, despite the fact that aromatic stack pairing aids in recognition of adenine at binding site, both the tyrosine residues of stack pairing play a crucial role in the stabilization of adenine at catalytic site. In the absence of both the tyrosine residues, adenine was unstable at catalytic site that results in the inhibition of N-glycosylation activity of gelonin protein. Hence, this study highlights the importance of π–π stack pairing in the N-glycosidic activity of gelonin by determining its role in stabilizing adenine at catalytic site.

1. Introduction

Ribosome inactivating proteins (RIPs) inhibit protein synthesis via the catalytic cleavage of N-glycosidic bond in the 28S ribosomal RNA of the larger subunit in eukaryotic ribosomes [1]. RIPs cleave the N-glycosidic bond and depurinate the isolated DNA, RNA, PolyA and intact ribosome. However, the activity of each RIP varies widely from substrate to substrate [2,3]. Based on their structure, RIPs have been divided into two categories: type I RIPs and type II RIPs. Type I RIPs have a single polypeptide chain that performs enzymatic function [1,4]. Type II RIPs are heterodimeric proteins with two polypeptide chains (chain A and chain B) linked by disulfide bonds; chain A is similar to that of the type I RIPs and responsible for the enzymatic function of type II RIPs while chain B is a galactose binding lectin responsible for binding on the surface of eukaryotic cells and retrograde transport of chain-A to cytosol [1,4]. More recently a type III RIP was introduced, including a single RIP from maize, in which the catalytic chain has an additional peptide tail that must be removed for the RIP to be active [5].

The present study employed gelonin protein – a type-I RIP, as a model to study the RIPs. Gelonin was reported from the seeds of *Gelonium multiflorum* and is a 31 kDa single chain type-I RIP [6]. Gelonin has been reported as a potent inactivator of protein synthesis in the mammalian cell-free translation system, but less toxic to intact cells due to its inability in binding to cells and in penetrating the cell membrane [7]. It has been reported with anti-HIV as well as anti-tumor activity [6–8]. It inhibits not only the *de novo* HIV-1 infection and cell-to-cell transmission of the virus, but also the viral replication in pre-infected cells [8]. Gelonin has also been proved to be an effective antiviral protein against Herpes Simplex Viruses and Human Herpes Virus-8 [9].

All proteins of the RIP family share almost a similar active site with conserved residues as well as conserved hydrogen bonds. Conserved arginine, glutamic acid and two tyrosine residues forming an aromatic–aromatic stack pairing are the hall mark residues of the active site of RIPs. Mechanism of N-glycosylation by RIPs has been proposed in earlier studies. In trichosanthin (type-I RIP from a plant *Trichosanthes kirilowii*), it is suggested that, conserved arginine of active site protonates the adenine at active site and is a crucial residue for the activity of trichosanthin [10]. It has also been proposed that RIPs have different substrate binding site and catalytic sites [11]. The substrate is first recognized by the aromatic–aromatic stack pairing at substrate binding site, while catalysis occurs at slightly different loci from substrate binding site. Role of conserved arginine, glutamate and tyrosine has been studied by mutagenesis and found to play a crucial role in the functioning of RIPs. However, the role of tyrosine residues of aromatic–aromatic stack pairing at catalytic site is still not clear. It has been proposed that aromatic–aromatic stack pairing plays important role in stabilization of substrate at substrate binding site. But, the stack pairing may also contribute to the movement of substrate from binding site to catalytic site and stabilizing adenine at catalytic site in addition to the stabilization of substrate (AMP) at

* Corresponding author. Fax: +91 4565 229334.
E-mail address: sk_pandian@rediffmail.com (S. Karutha Pandian).

0006-291X/$ - see front matter © 2011 Elsevier Inc. All rights reserved.
doi:10.1016/j.bbrc.2011.05.107

substrate binding site. In the present study, the role of aromatic–aromatic stack pairing in the stabilization of adenine at catalytic site of gelonin protein was analyzed.

2. Materials and methods

2.1. Preparation of protein complex

X-ray crystallographic structure of adenine bound gelonin complex (3KTU) has been used as an initial structure, which is a homodimer with a N-glycosylated adenine bound at its catalytic site. Water molecules have no role in salt bridge interaction at catalytic site, which has been inferred by removing all the water molecules along with a chain of 3KTU complex during the protein preparation step. The structure has been optimized by the addition of hydrogen atoms using Schrödinger's maestro interface [12]. Schrödinger's Protein Preparation Wizard [13] has been used for the removal of bad contacts, optimization of bond lengths and also to prepare the receptor model. Model prepared was then used to generate three mutant structures Y72A, Y113A, and a structure with both the mutation Y72A and Y113A using Schrödinger's maestro interface.

2.2. Glide scoring and Prime/MMGBSA free energy

Prime/MMGBSA method [14–16] has been used to score the free energy of binding of all the receptor–adenine complexes. All the complexes were scored using Glide XP [17] docking protocol without actually docking adenine with gelonin receptor. To achieve that, adenine has been extracted from the complex to be used as a ligand for docking and was prepared using LigPrep's [18] ligand preparation protocol. Grid of each complex was generated around the catalytic site by taking adenine as a reference molecule. Prepared adenine molecule has been docked with the complexes using generated grids. Obtained docking poses were then used for the calculation of free energy of binding by Prime/MMGBAS method.

The docked poses were minimized using the local optimization feature of Prime [14]. OPLS-AA force field [19,20] and GB/SA continuum solvent model were used to calculate the energies of the complexes. The binding free energy $\Delta G_{\text{binding}}$ is then estimated using an equation:

$$\Delta G_{\text{binding}} = E_{\text{R:L}} - (E_{\text{R}} + E_{\text{L}}) + \Delta G_{\text{solv}} + \Delta G_{\text{SA}}$$

where $E_{\text{R:L}}$ is the energy of complex, $E_{\text{R}} + E_{\text{L}}$ is sum of the energies of the receptor and ligand, ΔG_{solv} (ΔG_{SA}) is the difference between GBSA solvation energy (surface area energy) of complex and sum of the corresponding energies for the ligand and protein.

2.3. Molecular dynamic simulations

A molecular dynamics simulation approach has been followed to determine the effect of mutations on the stability of adenine at catalytic site [21]. All wild and mutant types of the complexes were subjected for 10 ns molecular dynamic simulation (MD simulation) using Desmond Molecular Dynamics System [22,23] with OPLS all-atom force field 2005 [19,20]. Desmond set up wizard has been used to prepare protein complex systems for MD simulations. Each one of the systems was then neutralized using an appropriate number of ions and then surrounded by an octahedral periodic box of SPC water molecules. The distance between box wall and protein complex was set to be greater than 5 Å, so that the protein did not directly interact with its own periodic image. Minimization of all prepared systems for MD simulation has been performed up to the maximum of 3000 steps using the method steepest descent until a gradient threshold (25 kcal/mol/Å) was reached. Minimized systems were used to run for 10 ns MD simulations at constant temperature of 300 K and constant pressure of 1 atm with a time step of 2 fs. Long range electrostatic interactions during the MD simulations were calculated using smooth particle Mesh-Ewald method. A 9 Å cutoff radius value has been used for coulombic short range interaction cutoff method.

2.4. Analysis of simulations

The root means square deviation (RMSD) of all the atoms has been calculated through the simulation, with the first frame as reference. The last 6 ns of the simulations were considered as production stage and used for analysis of structural changes. The average structures were calculated from the production stage for both wild and mutant protein complexes. The hydrogen bonds were defined as hydrogen acceptor–donor atom distances of less than 3 Å and acceptor–H-donor angles of more than 120°. Graphs were plotted to show the distance between adenine and tyrosine residues of stack pairing. Distance between each atom of adenine and carbons of tyrosine residues were calculated manually and further used to draw the plots.

3. Results and discussion

RMSD of adenine with active site residues in wild type protein (Fig. 1A) suggests it is stable and consistent conformation throughout the 10 ns simulation time with a standard deviation value of 0.09 (Table 1). Consistent conformation of adenine over a long time scale simulation indicates the high structural stability of adenine at the catalytic site of wild protein. Mutation of tyrosine74 to alanine does not seem to affect the conformation of adenine with active site residues since the mutant Y74A has shown very less structural deviations along the 10 ns simulation (Fig. 1A). Similarly, mutation of tyrosine113 to alanine failed to have any impact on the stability of adenine and the conformation of adenine with active site residues was found to be stable around 0.5 Å during the course of simulation (Fig. 1A). Trajectories of both Y74A and Y113A mutant type proteins were deviated by 0.10 and 0.16 Å, respectively (Table 1). The data suggests that mutation of any single tyrosine residue of π–π stack paring has no significant effect on the stability of adenine at the catalytic site. However, Y113A mutant shows deviation little higher as compared to that of Y74A. At the same time, stability of adenine was affected significantly at the catalytic site in double mutated system. After 2.5 ns the conformation of adenine with active site residues of the double mutated system has been altered significantly with an approximate RMSD of 1.5 Å (Fig. 1A) which persisted till the end of 10 ns simulation time during which adenine acquired a different conformation at catalytic site.

RMSD of wild and mutant protein backbones indicate the structural fluctuations in the backbone of proteins during the time series (Fig. 1B). The backbone of wild type protein has a standard deviation of less than 2 Å, indicating the superior quality of simulation (Table 1). Both the single mutant proteins have shown almost similar deviations as of wild type that explains the mutation of tyrosine to alanine has no change on the protein backbone (Fig. 1B). However, in double mutant, standard deviation in the backbone was slightly higher as compared to that of wild type protein.

On the basis of conserved H-bond between N3 of adenine and guanidium of Arg169, Ren et al. [24] has proposed N3 of adenine as the most likely protonation site for N-glycosylation [24]. The mechanism has been further supported by the study of Guo et al. [11] which states that the absence of H-bond between N3 of adenine and Arg169 results in the loss of N-glycosylation activity of

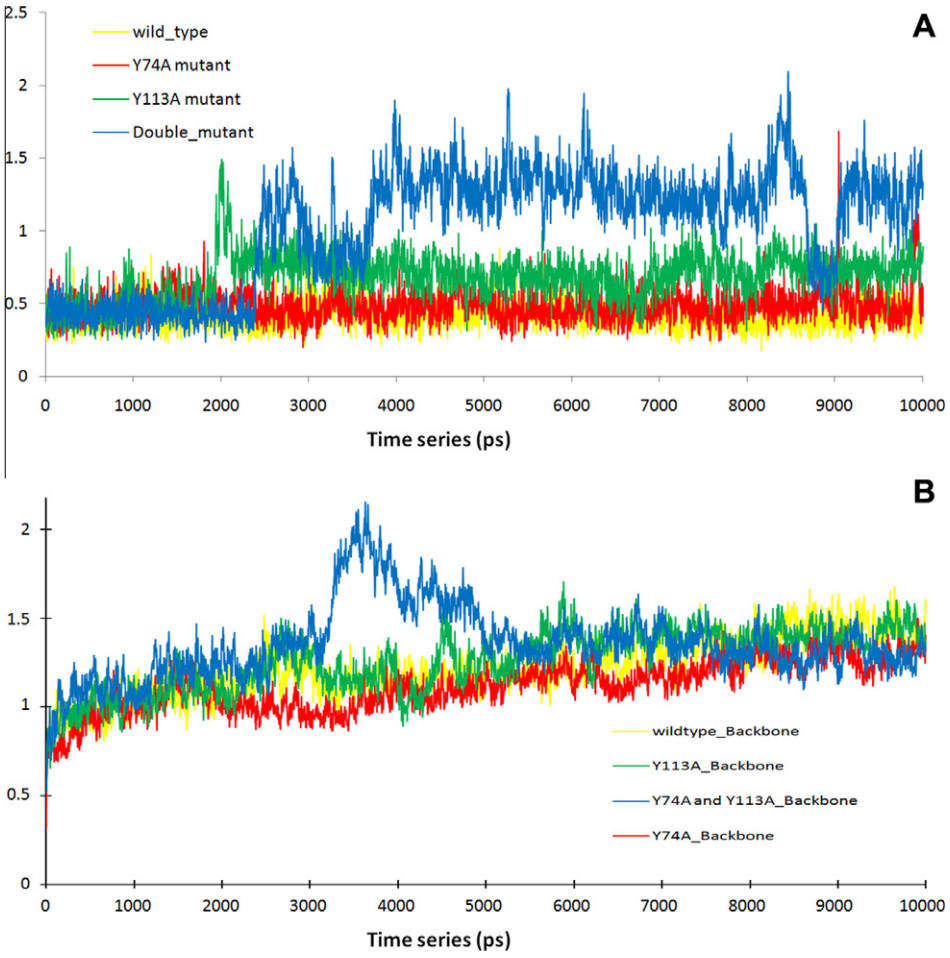

Fig. 1. (A) RMSD of adenine with active site residues during the simulation in wild and mutated systems. (B) RMSD of backbone of wild and mutated systems during the simulation.

Table 1
RMSD values of backbone and adenine with active site residues (Val75, Gly111, and Arg169) during the simulation in wild and mutant proteins.

Structure	RMSD (Å) of backbone	RMSD (Å) of adenine with active site residues
Wild type	0.16	0.09
Y74A mutant	0.14	0.10
Y113A mutant	0.17	0.16
Y74A and Y113A mutant	0.21	0.39

gelonin. Other conserved H-bonds with Gly111 and Val75 also play a crucial role in the stabilization of adenine. In wild type and single mutant proteins all the conserved H-bonds of adenine with active site residues were found stable during the 10 ns simulation (Table 2, Figs. S1 and S2). Hence, we report that mutation of tyr74 or tyr113 one at a time will not bring any significant change in the stability of adenine at catalytic site, since, in both the single mutants all adenine associated conserved H-bonds were stable with approximately similar bond length to that of wild type protein. Whereas, mutation of both the tyrosine residues of π–π stack paring to alanine made adenine unstable at its active site, by virtue of which adenine losses its conserved H-bonds with Arg169 and Gly111 (Table 2, Fig. S3). In double mutant system, adenine formed a new H-bond with Asp89, through which it acquires a new conformation (Fig. 2). RMSD graph of double mutant system (Fig. 1A) clearly indicates that adenine acquires an altered conformation with the help of newly formed H-bond with Asp89 after 2.5 ns to the end of simulation (Figs. 2 and 3). Therefore, complete loss of π–π stack paring at the active site makes adenine unstable at catalytic site and leads to an altered conformation. Results have also shown that adenine loses two conserved H-bonds, one with

Table 2
Hydrogen bonds (distance between donor H and acceptor atoms) present in the average structures of wild and mutant proteins.

Structure	H-bonds					
	75Val (H)-N1 Ade (Å)	111Gly (O)-HN6 Ade (Å)	111Gly (H)-HN7 Ade (Å)	75Val (O)-HN6 Ade (Å)	169Arg (NH1)-N3 Ade (Å)	89Asp (O)-HN7 Ade (Å)
Wild type	1.92	Absent	1.64	Absent	2.04	Absent
Y74A mutant	1.89	Absent	1.62	2.44	1.89	Absent
Y113A mutant	1.91	2.32	1.67	2.37	1.91	Absent
Double mutant	2.11	Absent	Absent	2.31	Absent	1.64

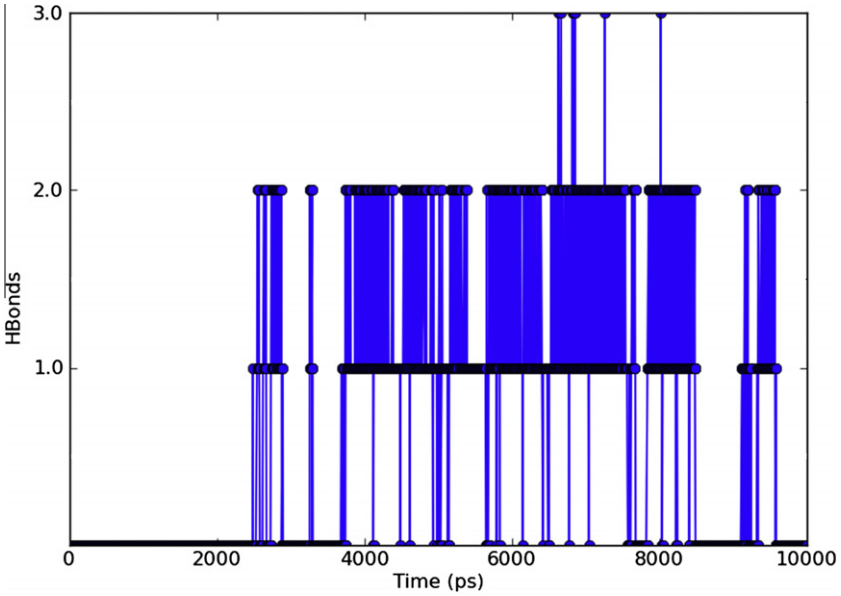

Fig. 2. Formation of new H-bond between adenine and Asp-89 after 2.5 ns simulation time.

Gly111 and another with Arg169 (Table 2), the most important H-bonds for N-glycosylation activity, that in turn corresponds to the reduced or complete loss of N-glycosidic activity of gelonin.

Even though, the tyrosine mutations have changed the conformation of adenine at catalytic site, there was no change in the protein structures. RMSD values of the secondary structures of mutant proteins were either less than that of the wild type protein or approximately same (Table 3). All the intra-hydrogen bonds in mutant proteins were conserved, similar to that of wild type protein [data not shown]. The average structures of wild and mutant proteins over the last 6 ns simulation time signify the major structural changes on an average scale. Superimposition of average structures reveal no change between the wild and mutant proteins (Fig. S4) while, the deviation of adenine from the catalytic site can be observed clearly in mutant proteins (Fig. 3A).

Mutation of single tyrosine residue of stack pairing has shown two types of structural changes at catalytic site depending on number of contacts or closeness with adenine ring. Single mutation either brought very minute structural change in another tyrosine residue of stack pairing or it made adenine to adjust its position slightly. Distance between adenine and tyrosine has been used as a scale to identify the structural changes at catalytic site and these structural changes were detected by comparing the distance between adenine and tyrosine in wild and mutant proteins (Fig. 4). Fig. 4C and E shows the distances between carbons of tyrosine residue and atoms of adenine in wild and mutant proteins. The distances were represented by solid line for wild type protein, whereas dotted lines for mutant proteins. Three different colors represent three different carbons of tyrosine. The solid line below the dotted line of the respective color indicates the closer association of adenine and tyrosine ring in wild type, i.e. tyrosine is located closer to adenine in wild type as compared to the mutant protein. Whereas, the solid line above the dotted line indicates that the tyrosine of mutant protein was located closer to adenine as compared to that of wild type protein. In Y113A mutant, solid lines were found below the dotted lines (Fig. 4C) and it is clear that tyrosine74 acquires a different conformation (shifts 11° away from adenine) in Y113A mutant as compared with wild type protein (Fig. 4B). The results explain the basis of stability of adenine at catalytic site even after the mutation of tyrosine113. Among the tyrosine residues of stack pairing, tyrosine74 has been found to be a stronger participant of stack pairing, since, mutation of tyrosine113 could have brought an unbalance at catalytic site. But, the loss of weak interaction at the opposite side of adenine with respect to tyrosine74 has been complemented by an increase in distance between tyrosine74 and adenine. In Y74A mutant, solid lines were above the dotted lines (Fig. 4E) and it is clear from that the adenine shifts slightly towards tyrosine113 as compared to that of wild type protein (Fig. 4D). The result explains the basis of stability of adenine at catalytic site even after the mutation of tyrosine74. In this case, loss of strong interaction at opposite side of

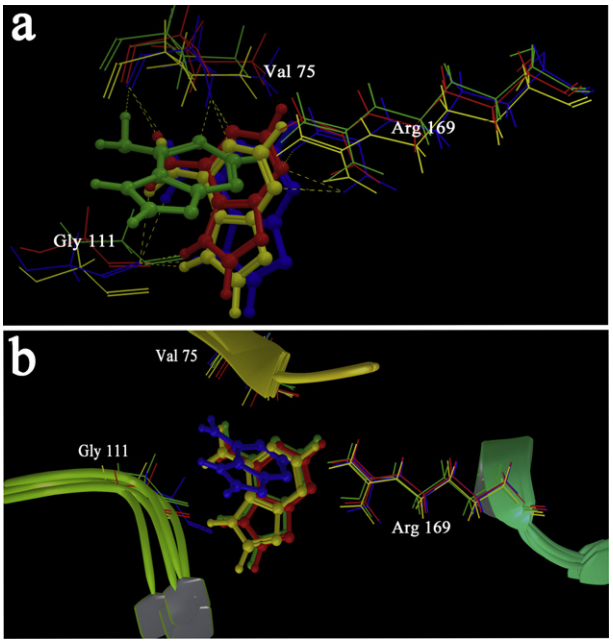

Fig. 3. (A) Superimposed last frames of wild type protein (yellow), mutated Y74A (red), mutated Y113a (blue), and double mutated (green) systems. (B) Superimposed average structures (over last 6 ns simulation) of wild type protein (yellow), mutated Y74A (red), mutated Y113a (green), and double mutated (blue) systems. (For interpretation of the references to color in this figure legend, the reader is referred to the web version of this article.)

Table 3
RMSD values of secondary structures of wild and mutant proteins during the simulation.

Structure	RMSD of helix (Å)	RMSD of strand (Å)	RMSD of loop (Å)
Wild type	0.23	0.13	0.21
Y74A mutant	0.14	0.17	0.23
Y113A mutant	0.19	0.16	0.23
Y74A and Y113A mutant	0.12	0.10	0.26

adenine has been complemented by a shift in adenine towards tyrosine113 decreasing its distance with tyrosine113.

Simulation studies performed, were further supported by the docking scores and free energy calculations. Binding energy was calculated using the Prime MM-GBSA method and small molecule at active site has been scored by Glide XP docking (Table 4). The intermolecular van der Waals interactions (ΔE_{vdw}) for Y74A and Y113A were almost the same but lesser than the wild protein. While ΔE_{vdw} of double mutated protein is much lower than the wild type protein as well as other single mutant proteins. The van der Waals energy values indicate that the loss of both the tyrosine residues weakened the electrostatic interactions around the catalytic site of gelonin which further validates the structural analysis explained above. Significant difference between the free energies of binding of wild type and mutant proteins were found such as the double mutant has a total of −17.23 kcal mol^{-1} binding energy $\Delta G_{binding}$, which was 9.68 kcal mol^{-1} higher than that of wild type protein. Similarly, double mutant protein has also shown very low docking score explaining the instability of adenine at catalytic site. The above mentioned free energy values and docking scores

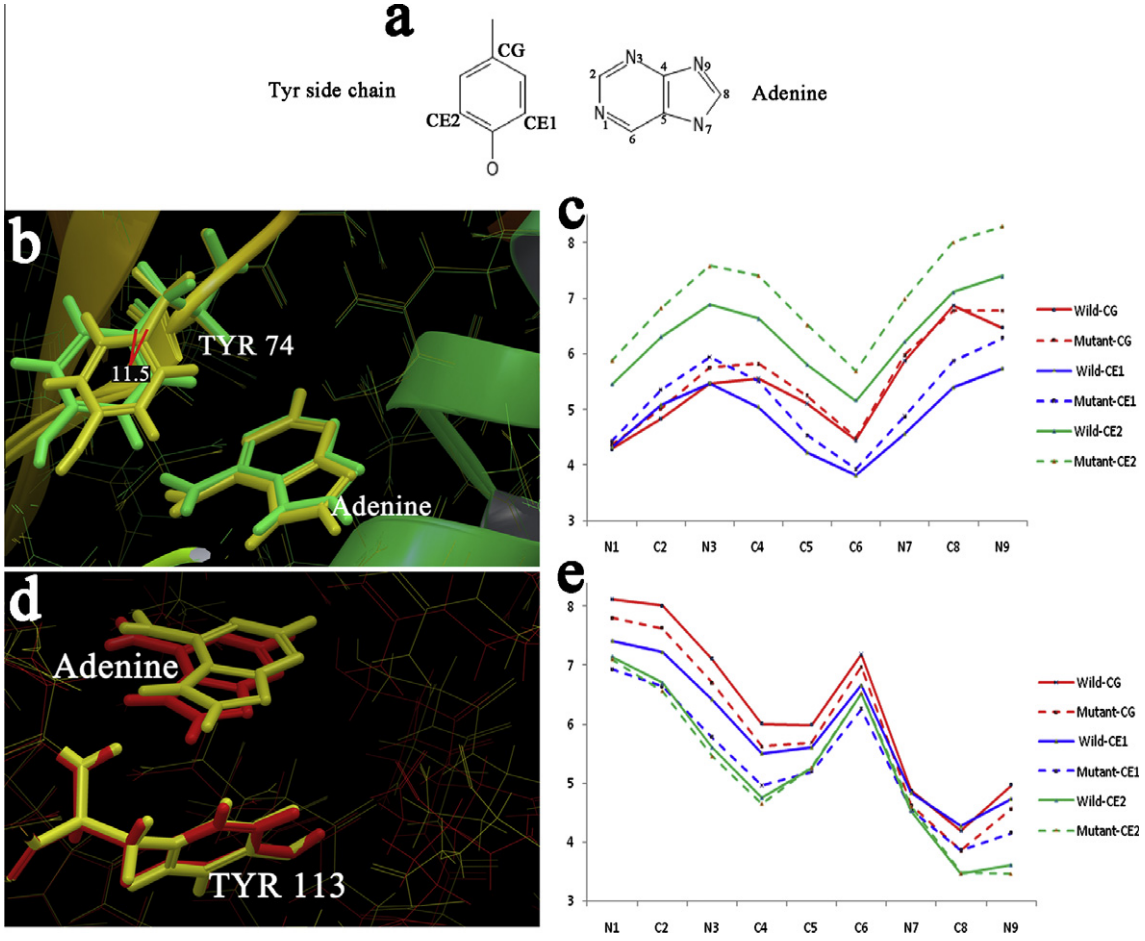

Fig. 4. (A) Labeled adenine and side chain of tyrosine. Labels marked were used in measuring the distances between adenine and tyrosine carbons. (B) Superimposed catalytic site of wild type and mutated Y113A proteins illustrate the shift of tyrosine74 side chain towards adenine in the absence of tyrosine113. (C) Graph showing the distances between the carbon atoms of tyrosine74 and adenine. (D) Superimposed catalytic site of wild type and mutated Y74A proteins illustrate the shift of adenine towards tyrosine113 side chain residue in the absence of tyrosine74. (E) Graph showing the distances between the carbon atoms of tyrosine113 and adenine.

Table 4
Docking scores and energies (kcal/mol) of the wild and mutated complexes.

Structure	Glide XP score	Free energy of binding (Prime MM GBSA)	Ligand strain energy	Glide $E_{van\ der\ Waals}$
Wild type	−8.27	−26.91	0.92	−19.91
Y113A mutant	−7.96	−21.51	1.25	−17.53
Y74A mutant	−5.04	−17.31	1.29	−17.10
Double mutant	−4.61	−17.23	0.96	−14.70

show the complete loss of π–π stack pairing from the active site resulting in a less energy favored association and makes adenine unstable at catalytic site. Ligand strain energies of complexes show the strains on adenine at catalytic site and suggest that absence of any one of the tyrosine from the π–π stack pairing increases the strain on adenine at catalytic site that in turn reduces the N-glycosidic activity of gelonin which has been further supported by the higher free energies of single mutant proteins and lower docking scores, demonstrating an energetically unfavorable mutation.

In the present study the structural insight of gelonin protein's catalytic site and the effect of *in silico* mutations of tyrosine rings on it were analyzed using computational methods such as MD simulations, docking, and MM GBSA free energy calculation. In the mutants Y74A and Y113A, all the conserved H-bonds were stable similar to that of the wild type protein and Arg169 still holds the ability to form H-bond with N3 of adenine. But, the docking studies and free energy analysis of these mutated systems indicates that the above mentioned mutations made adenine less energetically favorable at catalytic site. Hence, it is concluded that the mutation of any single tyrosine residue may cause slight decrease in N-glycosylation of adenine at catalytic site, without much change in their structure. Mutation of both the tyrosine residues of π–π stack pairing system leads to an altered configuration of adenine at the catalytic site of gelonin, significantly increasing the free energy of binding and decreasing the docking score of adenine at catalytic site. This study clearly emphasizes that at least one of the tyrosine residues of π–π stack pairing system is essential for the N-glycosylation activity of gelonin and both the tyrosine residues of π–π stack pairing system stabilizes the adenine with minimum strain on it.

Acknowledgments

Authors acknowledge the computational facilities provided by the Bioinformatics Infrastructure Facility (funded by Department of Biotechnology, Government of India; Grant No. BT/BI/25/001/2006), Alagappa University, Karaikudi.

Appendix A. Supplementary data

Supplementary data associated with this article can be found, in the online version, at doi:10.1016/j.bbrc.2011.05.107.

References

[1] L. Barbieri, M. Ciani, T. Girbes, W.Y. Liu, E.J. Van Damme, W.J. Peumans, F. Stirpe, Enzymatic activity of toxic and non-toxic type 2 ribosome-inactivating proteins, FEBS Lett. 563 (2004) 219–222.

[2] L. Barbieri, P. Valbonesi, E. Bonora, P. Gorini, A. Bolognesi, F. Stirpe, Polynucleotide: adenosine glycosidase activity of ribosome-inactivating proteins: effect on DNA RNA and poly(A), Nucleic Acids Res. 25 (1997) 518–522.

[3] T.K. Amukele, V.L. Schramm, Ricin A-chain substrate specificity in RNA DNA and hybrid stem–loop structures, Biochemistry 43 (2004) 4913–4922.

[4] E.J. Van Damme, A. Barre, L. Barbieri, P. Valbonesi, P. Rouge, F. Van Leuven, F. Stirpe, W.J. Peumans, Type 1 ribosome-inactivating proteins are the most abundant proteins in iris (*Iris hollandica*var. Professor Blaauw) bulbs: characterization and molecular cloning, Biochem. J. 324 (1997) 963–970.

[5] E.J.M. Van Damme, Q. Hao, Y. Chen, A. Barre, F. Vandenbussche, S. Desmyter, P. Roug, W.J. Peumans, Ribosome-inactivating proteins: a family of plant proteins that do more than inactivate ribosomes, Crit. Rev. Plant Sci. 20 (2001) 395–465.

[6] S. Lee-Huang, H.F. Kung, P.L. Huang, B.Q. Li, P. Huang, H.I. Huang, H.C. Chen, A new class of anti-HIV agents: GAP31 DAPs 30 and 32, FEBS Lett. 291 (1991) 139–144.

[7] Z. Li, Y. Qu, H. Li, J. Yuan, Truncations of gelonin lead to a reduction in its cytotoxicity, Toxicology 231 (2007) 129–136.

[8] H.G. Li, P.L. Huang, D. Zhang, Y. Sun, H.C. Chen, J. Zhang, X.P. Kong, S. Lee-Huang, A new activity of anti-HIV and anti-tumor protein GAP31:DNA adenosine glycosidase-structural and modeling insight into its functions, Biochem. Biophys. Res. Commun. 391 (2010) 340–345.

[9] Y. Sun, P.L. Huang, J.J. Li, Y.Q. Huang, L. Zhang, S. Lee-Huang, Anti-HIV agent MAP30 modulates the expression profile of viral and cellular genes for proliferation and apoptosis in AIDS-related lymphoma cells infected with Kaposi's sarcoma-associated virus, Biochem. Biophys. Res. Commun. 287 (2001) 983–994.

[10] P.C. Shaw, K.M. Lee, K.B. Wong, Recent advances in trichosanthin a ribosome-inactivating protein with multiple pharmacological properties, Toxicon 45 (2005) 683–689.

[11] Q. Guo, W. Zhou, H.M. Too, J. Li, Y. Liu, M. Bartlam, Y. Dong, K.B. Wong, P.C. Shaw, Z. Rao, Substrate binding and catalysis in trichosanthin occur in different sites as revealed by the complex structures of several E85 mutants, Protein Eng. 16 (2003) 391–396.

[12] Maestro, Version 9.1, Schrödinger, LLC, New York, NY, 2010.

[13] Schrödinger Suite 2009 Protein Preparation Wizard; Epik Version 2.0, Schrödinger, LLC, New York, NY, 2009; Impact Version 5.5, Schrödinger, LLC, New York, NY, 2009; Prime Version 2.1, Schrödinger, LLC, New York, NY, 2009.

[14] Prime, Version 2.2, Schrödinger, LLC, New York, NY, 2010.

[15] M. Srivastava, H. Sing, P.K. Naik, Molecular modeling evaluation of the antimalarial activity of artemisinin analogues: molecular docking and rescoring using Prime/MM-GBSA approach, Curr. Res. J. Biol. Sci. 2 (2010) 83–102.

[16] H.S. Lee, J. Choi, S. Yoon, Evaluation of advanced structure-based virtual screening methods for computer-aided drug discovery, Genomics Inform. 5 (2007) 24–29.

[17] R.A. Friesner, J.L. Banks, R.B. Murphy, T.A. Halgren, J.J. Klicic, D.T. Mainz, M.P. Repasky, E.H. Knoll, M. Shelley, J.K. Perry, D.E. Shaw, P. Francis, P.S. Shenkin, Glide: a new approach for rapid accurate docking and scoring 1 method and assessment of docking accuracy, J. Med. Chem. 47 (2004) 1739–1749.

[18] LigPrep, Version 2.4, Schrödinger, LLC, New York, NY, 2010.

[19] W.L. Jorgensen, D.S. Maxwell, J. Tirado-Rives, Development and testing of the OPLS all-atom force field on conformational energetics and properties of organic liquids, J. Am. Chem. Soc. 118 (1996) 11225–11236.

[20] G.A. Kaminski, R.A. Friesner, J. Tirado-Rives, W.L. Jorgensen, Evaluation and reparametrization of the OPLS-AA force field for proteins via comparison with accurate quantum chemical calculations on peptides, J. Phys. Chem. B 105 (2001) 6474–6487.

[21] H. Sun, Y.J. Jiang, Q.S. Yu, C.C. Luo, J.W. Zou, Effect of mutation K85R on GSK-3beta: molecular dynamics simulation, Biochem. Biophys. Res. Commun. 377 (2008) 962–965.

[22] Desmond Molecular Dynamics System, Version 2.4, D.E. Shaw Research, New York, NY, 2010. Maestro–Desmond Interoperability Tools, Version 2.4, Schrödinger, New York, NY, 2010.

[23] Z. Guo, U. Mohanty, J. Noehre, T.K. Sawyer, W. Sherman, G. Krilov, Probing the alpha-helical structural stability of stapled p53 peptides: molecular dynamics simulations and analysis, Chem. Biol. Drug. Des. 75 (2010) 348–359.

[24] J. Ren, Y. Wang, Y. Dong, D.I. Stuart, The N-glycosidase mechanism of ribosome-inactivating proteins implied by crystal structures of alpha-momorcharin, Structure 2 (1994) 7–16.